Cysteine Conformation and Sulfhydryl Interactions in Proteins and Viruses. 2. Normal Coordinate Analysis of the Cysteine Side Chain in Model Compounds†

Huimin Li,‡ Charles J. Wurrey,§ and George J. Thomas, Jr.*,‡

Contribution from the Division of Cell Biology and Biophysics, School of Biological Sciences, University of Missouri—Kansas City, Kansas City, Missouri 64110. *Received December 23, 1991*

Abstract: We report vibrational normal mode analyses of cysteine and several model mercaptans containing the $-CHRCH_2SH$ group (R = H or CH_3). The results provide a basis for assigning observed Raman frequencies to specific conformers of the cysteinyl C_α–C_β–S–H side chain and for assessing SH hydrogen bonding with appropriate donor and acceptor groups. Vibrational spectra and normal coordinate analyses of L-cysteine, 1-propanethiol (1PT), 1-propanedeuteriothiol (1PT-d_1), and 2-methyl-1-propanethiol (2M1PT) and corresponding experimental data on 2-methyl-2-propanethiol derivatives (2M2PT and 2M2PT-d_1) indicate that conformation-sensitive modes occur in both the C–S stretching ($600 < \sigma_{CS} < 800$ cm^{-1}) and the S–H stretching ($2500 < \sigma_{SH} < 2650$ cm^{-1}) regions of the Raman spectrum. Using a generalized valence force field, we have correlated the side-chain torsion angle (X^1) of the C_α–C_β bond with σ_{CS}, and the torsion angle (X^2) of the C_β–S bond with both σ_{CS} and σ_{SH}. The principal conclusions from the present study are as follows: (i) The force field obtained from 1PT is satisfactorily transferable to 2M1PT and L-cysteine and reproduces the observed trends for σ_{SH} and σ_{CS} of these molecules. (ii) σ_{CS} can be shifted substantially (up to 50 cm^{-1}) by changes in X^1, but is less sensitive (<10 cm^{-1}) to changes in X^2. (iii) σ_{SH} is perturbed sufficiently by changes in X^2 to account for previously reported frequency differences in Raman SH bands of cysteinyl gauche rotamers.[1] Correlations are proposed for the dependence of both σ_{CS} and σ_{SH} upon conformation of the C_α–C_β–S–H network. These correlations are expected to be useful for determining cysteine side-chain environments in proteins and their assemblies, including virions and viral precursors.

Introduction

The thiol group (SH) of cysteine is capable of donating and accepting intramolecular hydrogen bonds which contribute to the stabilization of native protein structures.[2-5] A recent survey[6] of crystallographic structures in the Brookhaven Protein Data Bank indicates that 72% of cysteine SH groups participate in S–H···O or S–H···N contacts of less than 4 Å. In the majority of cases (62%) the acceptor is a carbonyl oxygen. About half of all cysteines are located in domains of α-helical secondary structure, in which the SH group at position i is capable of donating a hydrogen bond to the peptide carbonyl of residue i-4, provided that the side-chain C_α–C_β torsion (X^1, Figure 1) is approximately −60° (gauche$^-$ rotamer). Similarly, cysteine residues just beyond the C-terminus of an α-helix can form a side-chain to main-chain hydrogen bond, supplanting a main-chain NH···O=C linkage and thus serving to "cap" the α-helix.[6,7] The distribution of cysteine residues in proteins with respect to the side-chain C_β–S torsion (X^2, Figure 1) has also been studied, indicating a preference for the gauche$^+$ range (60–80°).[3] Collectively, these analyses reveal a variety of rotamer conformations and hydrogen-bonding environments accessible to the cysteine side chain, including configurations which may play a role in defining boundaries of α-helix formation during protein folding.

Cysteine side-chain conformations and hydrogen-bonding interactions in selected proteins have been assessed by surveying neutron and X-ray crystallographic data.[6] However, other methods are required to probe cysteine interactions which are defined only for noncrystalline proteins, including aqueous protein solutions. Examples are the thiols of membrane proteins, which act as intra- or intercellular antioxidants by scavenging free radicals,[8] and the reduced forms of thioredoxin and glutaredoxin, which serve ubiquitously as protein disulfide reductases.[9] Raman spectroscopy offers several advantages for probing such cysteine interactions, including its capability for detecting SH Raman markers in both solution and crystal structures, its suitability for monitoring deuterium exchange dynamics of the SH group, and its relatively rapid data collection and analysis protocols.

Recently, we reported a correlation of the Raman S–H stretching frequency (σ_{SH}) with hydrogen-bonding donor and acceptor interactions of the thiol group in cysteine model compounds.[1] Other investigators have noted the sensitivity of the Raman C_βS stretching frequency (σ_{CS}) to conformation of the cysteine side chain.[10,11] In the present work, we report Raman spectra of normal and deuterated cysteine model compounds and describe normal coordinate calculations performed on L-cysteine, 1-propanethiol (1PT), 1-propanedeuteriothiol (1PT-d_1), and 2-methyl-1-propanethiol (2M1PT), using a refined valence force field. The results indicate correlations of the cysteine side-chain torsion X^1 with the Raman C_βS stretching frequency, and of the torsion X^2 (Figure 1) with both σ_{CS} and σ_{SH}. These correlations have not been recognized previously. The present study extends earlier work by providing a basis for understanding the conformational dependence of Raman S–H and C–S stretching vibrations of the cysteine moiety. The results are expected to facilitate structural interpretation of Raman bands assigned to cysteine residues of proteins. Additionally, these results should be useful for interpreting changes observed in Raman SH bands of viral proteins in different assembly states.[12,13]

Materials and Methods

1. Materials. The mercaptans 1-propanethiol (1PT) and 2-methyl-1-propanethiol (2M1PT) were purchased from Aldrich. 1-Propane-

* Author to whom correspondence may be addressed.

† Part XXXVI in the series Structural Studies of Viruses by Laser Raman Spectroscopy; supported by NIH Grant AI11855 (G.J.T.).

‡ Division of Cell Biology and Biophysics, School of Biological Sciences.
§ Department of Chemistry, College of Arts and Sciences.

(1) Li, H.; Thomas, G. J., Jr. *J. Am. Chem. Soc.* **1991**, *113*, 456–462.
(2) Kollman, P.; McKelvey, J.; Johansson, A.; Rothenberg, S. *J. Am. Chem. Soc.* **1975**, *97*, 955–965.
(3) Ippolito, J. A.; Alexander, R. S.; Christianson, D. W. *J. Mol. Biol.* **1990**, *215*, 457–471.
(4) Burley, S. K.; Petsko, G. A. *Adv. Protein Chem.* **1988**, *39*, 125–189.
(5) McGrath, M. E.; Wilke, M. E.; Higaki, J. N.; Craik, C. S.; Fletterick, R. J. *Biochemistry* **1989**, *28*, 9264–9270.
(6) Gregoret, L. M.; Rader, S. D.; Fletterick, R. J.; Cohen, F. E. *Proteins: Struct. Funct. Genet.* **1991**, *9*, 99–107.
(7) Presta, L. G.; Rose, G. D. *Science* **1988**, *240*, 1632–1641.
(8) Frei, B.; Stocker, R.; Ames, B. N. *Proc. Natl. Acad. Sci. U.S.A.* **1988**, *85*, 9748–9752.
(9) Holmgren, A. *J. Biol. Chem.* **1989**, *264*, 13963–13966.
(10) Kuptsov, A. H.; Trofimov, V. I. *J. Biomol. Struct. Dyn.* **1985**, *3*, 185–196.
(11) (a) Nogami, N.; Sugeta, H.; Miyazawa, T. *Chem. Lett.* **1975**, 147–150. (b) Nogami, N.; Sugeta, H.; Miyazawa, T. *Bull. Chem. Soc. Jpn.* **1975**, *48*, 2417–2420.
(12) Thomas, G. J., Jr.; Li, Y.; Fuller, M. T.; King, J. *Biochemistry* **1982**, *21*, 3866–3878.
(13) Li, T.; Chen, Z.; Johnson, J. E.; Thomas, G. J., Jr. *Biochemistry* **1990**, *29*, 5018–5026.

0002-7863/92/1514-7463$03.00/0

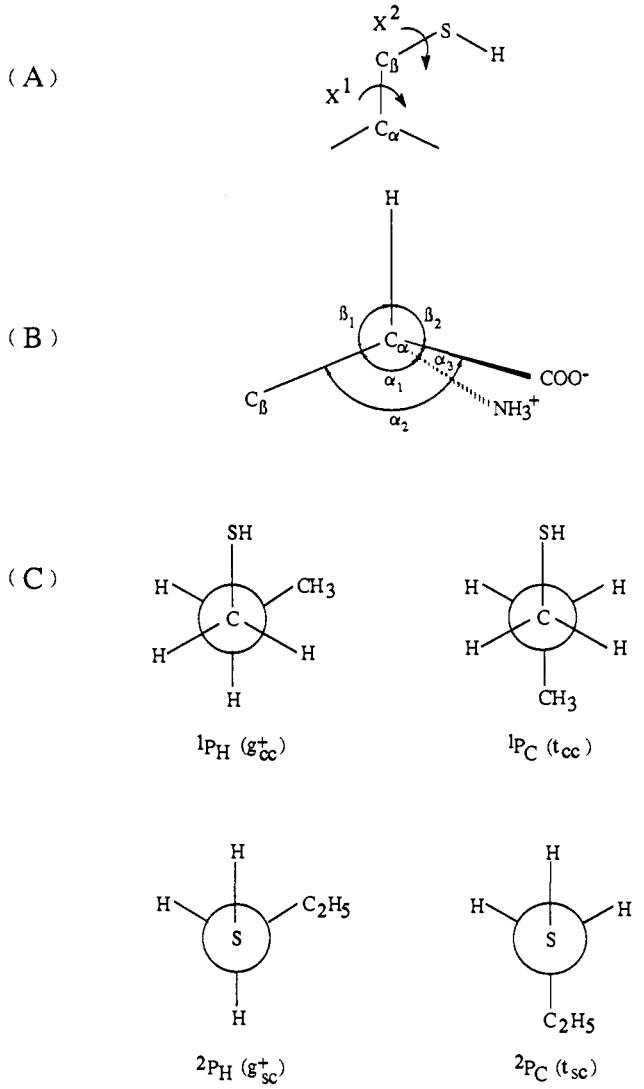

Figure 1. (A) Torsion angles of the cysteine side chain. (B) Internal coordinates of the cysteine C_α linkages. (C) Rotamers ^1P_H, ^2P_H, ^1P_C, and ^2P_C of 1-propanethiol. P_H designates the thiol hydrogen in the trans orientation with respect to a hydrogen substituent on the adjoining methylene carbon. P_C designates the trans orientation of the methyl carbon with respect to SH. The superscript prefix (1 or 2) indicates the relevant torsion angle (X^1 or X^2), as well as the number of bonds separating the dihedral linkage from the peptide carbon (C_α).

deuteriothiol (1PT-d_1, 95%) and 2-methyl-2-propanedeuteriothiol (2M2PT-d_1, 95%) were prepared by stirring 1PT and 2M2PT in D_2O for 48 h at room temperature. All mercaptans were freshly distilled and chromatographed on a 15-cm column of baked alumina gel before use to remove traces of water or polar contaminants. The absence of impurities containing hydroxyl or amino groups was verified by Raman or infrared spectroscopy, as described.[14] Orthorhombic L-cysteine was obtained from Sigma, and its crystal structure[15] was verified by X-ray diffraction (courtesy of Professor A. H.-J. Wang, University of Illinois, Urbana–Champaign).

2. Spectroscopy. Raman spectra were excited in the 90° scattering geometry with the 514.5-nm line of a Coherent Innova-70 argon ion laser, using approximately 100 mW of radiant power at the sample. Samples were sealed in glass capillary tubes (Kimax #34507) maintained at ambient temperature (25 °C). Spectra in the interval 100–3500 cm^{-1} were recorded on a Spex Ramalog 1401 spectrometer under the control of an IBM microcomputer. Data were collected at intervals of either 0.5 or 1.0 cm^{-1}, with an integration time of 1.0 s and spectral slit width of 1 cm^{-1}. Frequencies, listed in Table I, were calibrated using indene as a standard. Reported S–H and C–S group frequencies are accurate to within 1 cm^{-1} for strong or sharp bands.

Table I. Raman Frequencies and Assignments of 1-Propanethiol and 1-Propanedeuteriothiol

1-propanethiol		1-propanedeuteriothiol	
frequency	assignment (^1P_H)	frequency	assignment (^1P_H)
2967	CH_3 stretch	2964	CH_3 stretch
2967	CH_3 stretch	2964	CH_3 stretch
2932	CH_2 stretch	2933	CH_2 stretch
2932	CH_2 stretch	2933	CH_2 stretch
2874	CH_2 stretch	2874	CH_2 stretch
2874	CH_2 stretch	2874	CH_2 stretch
2856	CH_3 stretch	2856	CH_3 stretch
2589[a]	S–H stretch (^2P_C)		
2581[a]	S–H stretch	1876[a]	S–D stretch
1461	CH_2 scissor	1457	CH_2 scissor
1453	CH_3 deformation	1457	CH_3 deformation
1453	CH_3 deformation	1457	CH_3 deformation
1435	CH_2 scissor	1434	CH_2 scissor
1381	CH_3 deformation	1379	CH_3 deformation
1353	CH_2 wagging (^1P_C)	1353	CH_2 wagging (^1P_C)
1336	CH_2 wagging	1334	CH_2 wagging
1295	CH_2 wagging	1294	CH_2 wagging
1248	CH_2 twist	1244	CH_2 twist
1217	CH_2 twist	1213	CH_2 twist
1109	C–C stretch	1098	C–C stretch
1088	CH_3 rocking (^1P_C)	1082	CH_3 rocking (^1P_C)
1068	CH_3 rocking	1058	CH_3 rocking
1034	C–C stretch	1033	C–C stretch
923	CH_3 rocking	899	CH_3 rocking
896	CH_2 rocking	890	CH_2 rocking
876	CH_2 rocking (^1P_C)	854	CH_2 rocking (^1P_C)
816	C–S–H bend		
792	C–S–H bend (^1P_C)		
772	CH_2 rocking	793	CH_2 rocking
732	CH_2 rocking (^1P_C)	730	CH_2 rocking (^1P_C)
704	C–S stretch (^1P_C)		
650	C–S stretch	655	C–S stretch
		617	C–S–D bend
413	C–C–C bend	412	C–C–C bend
361	C–C–C bend (^1P_C)	361	C–C–C bend (^1P_C)
284	C–C–S bend	282	C–C–S bend
240	CH_3 torsion	240	CH_3 torsion
190[b]	C–S torsion	150[b]	C–S torsion
137	C–C torsion	120	C–C torsion

[a] Data from 1% 1PT and 1% 1PT-d_1 solutions (mol/mol) in CCl_4. [b] Data from ethanethiol and ethanedeuteriothiol (ref 28).

FTIR data were obtained from 400 to 4000 cm^{-1} with a Mattson Instruments Sirius 100 spectrometer. Usually, 800 scans each of the liquid sample and background were collected with spectral resolution of 8 cm^{-1} and a triangular apodization function. Liquids were contained in a variable-thickness cell with CaF_2 windows. Spectra of 1PT, 2PT, 2M1PT, and 2M2PT in the gas phase were obtained from the chromatographically pure liquids distilled at their ambient vapor pressure (<20 Torr) into an evacuated 10-cm cell with CsI windows. Gas-phase spectra were collected with 1-cm^{-1} spectral resolution.

3. Computational Methods. Normal coordinate calculations were performed on a Digital VAXstation 3100 operating under ULTRIX Version 4.2. We employed the program GZINT, based upon the GF-matrix formulation[16] and kindly provided by Professor Richard A. Mathies, Department of Chemistry, University of California, Berkeley. GZINT facilitates solution of the vibrational secular equations in either Cartesian or internal coordinates and is capable of adjusting an initial set of force constants to give a weighted least-squares fit of calculated frequencies. Potential energy distributions in terms of the valence force constants were calculated for each normal mode according to standard procedure. (The coefficients of the force constants represent the fractions that contributed to the total energy in the normal mode, using the relation $P_{\alpha m} = \sum\sum A_{\alpha i}A_{\alpha j}Z_{ijm}\phi_m\lambda_\alpha^{-1}$, where $A_{\alpha i}$ is the coefficient of symmetry coordinate i in normal mode α, λ_α is the eigenvalue, Z_{ijm} is the coefficient of force constant ϕ_m in element f_{ij} of the F matrix, and $\sum P_{am} = \lambda_a^{-1}\sum A_{ai}A_{aj}\sum Z_{ijm}\Phi_m = 1$).[17]

(14) Thomas, G. J., Jr. *Physical Techniques in Biological Research*, 2nd ed.; Oster, G. F., Ed.; Academic Press: New York, 1971; Vol. 1A, pp 277–346.
(15) Kerr, K. A.; Ashmore, J. P. *Acta Crystallogr.* **1973**, *B29*, 2124–2127.
(16) Wilson, E. B.; Decius, J. C.; Cross, P. C. *Molecular Vibrations*; McGraw-Hill: New York, 1955.
(17) Curry, B. U. Vibrational Analysis of Visual Pigment Chromophores. Ph.D. Thesis, University of California, Berkeley, 1983.

Table II. Diagonal Force Constants for L-Cysteine and Model Mercaptans

force constant	description	value
	All Molecules	
	Stretch, mdyn/Å	
$f(1)$	S–H	3.7970
$f(2)$	C–S	3.4693
$f(3)$	C–H (CH_3)	4.6795
$f(4)$	C–H (CH_2)	4.5895
$f(5)$	C–C	4.1973
	Bend, mdyn/rad^2	
$f(6)$	∠C–S–H	0.7112
$f(7)$	∠S–C–H	0.5197
$f(8)$	∠C–C–S	0.6638
$f(9)$	∠H–C–H (CH_2)	0.5406
$f(10)$	∠C–C–H	0.7331
$f(11)$	∠C–C–C	1.3952
$f(12)$	∠H–C–H (CH_3)	0.5372
	Torsion, mdyn/rad^2	
$f(13)$	HC–CC	0.1187
$f(14)$	CC–CS	0.1788
$f(15)$	CC–SH	0.0355
	Cysteine Only	
	Stretch, mdyn/Å	
$f(16)$	C–C (C–COO)	4.2035
$f(17)$	C–N	3.8970
$f(18)$	C–O	7.9231
$f(19)$	N–H	5.4078
	Bend, mdyn/rad^2	
$f(20)$	∠C–C–N	1.0547
$f(21)$	∠C–C–H (H–C–COO)	0.7102
$f(22)$	∠N–C–H	0.6522
$f(23)$	∠C–C–N (COO–C–N)	1.9484
$f(24)$	∠C–C–O	1.9408
$f(25)$	∠C–N–H	0.6765
$f(26)$	∠O–C–O	0.9932
$f(27)$	∠H–N–H	0.5653
	Torsion, mdyn/rad^2	
$f(28)$	CC–COO	0.0700
$f(29)$	HN–CC	0.0720
	Out-of-Plane Wag, mdyn/rad^2	
$f(30)$	∠CCO–O	0.9639

Table III. Off-Diagonal Force Constants for L-Cysteine and Model Mercaptans

force constant	description	value
	All Molecules	
	Stretch·Stretch, mdyn/Å	
$f(31)$	C–S, C–C	0.1874
$f(32)$	C–H, C–H	0.0134
$f(33)$	C–S, S–H	0.4352
$f(34)$	C–H, S–H	0.1429
	Stretch·Bend, mdyn/rad	
$f(35)$	C–C, ∠CCH	0.2859
$f(36)$	C–S, ∠CCH	0.1410
$f(37)$	C–C, ∠SCH	0.0660
$f(38)$	C–C, ∠CCC	−0.2213
$f(39)$	C–C, ∠CCS	0.4957
$f(40)$	C–S, ∠CCS	0.3505
$f(41)$	S–H, ∠CSH	−0.3350
$f(42)$	S–H, ∠SCH	0.3037
$f(43)$	S–H, ∠CCS	−0.2542
	Bend·Bend, mdyn/rad^2	
$f(44)$	∠CCH, ∠CCH	0.0028
$f(45)$	∠CCH, ∠CCH	0.0327
$f(46)$	∠SCH, ∠CCH	0.1639
$f(47)$	∠CCH, ∠CCS	−0.2801
$f(48)$	∠HCH, ∠CCH	0.0654
	2-Methyl-1-propanethiol Only	
	Stretch·Bend, mdyn/rad	
$f(49)$	C–S, ∠CCC	−0.2324
	Bend·Bend, mdyn/rad^2	
$f(50)$	∠CCC, ∠CCC	−0.3034
$f(51)$	∠CCC, ∠CCS	−0.2914
$f(52)$	∠CCC, ∠CCH (CH)	0.5152
	Cysteine Only	
	Stretch·Bend, mdyn/rad	
$f(53)$	C–O, ∠OCO	1.1160
$f(54)$	C–C, ∠OCO	−0.2296
$f(55)$	C–O, ∠CCO	1.2581
$f(56)$	C–O, ∠CSH	−0.3174
	Bend·Bend, mdyn/rad^2	
$f(57)$	∠CCC, ∠CCO	0.3500
$f(58)$	∠OCO, ∠CCO	0.3500

The G matrices were calculated from structural data obtained on L-cysteine by neutron diffraction[18] and on model mercaptans by microwave spectroscopy.[19-21] The following bond lengths and bond angles were determined for 1PT, 1PT-d_1, and 2M1PT: C–S 1.819 Å, methyl C–H 1.091 Å, S–H 1.335 Å, C–C 1.526 Å, methylene and methyne C–H 1.096 Å, ∠CSH 96.5°.[19-21] Dihedral angles were assumed to be 60°, and all other bond angles were assumed tetrahedral. For L-cysteine, the neutron diffraction studies give C–S 1.80 Å, C–N 1.488 Å, S–H 1.36 Å, and ∠CSH 97.0°.[18] On the basis of available experimental data,[11] we assumed the $^1P_H{}^2P_H$ rotamer of 1PT to be the most stable. Frequencies were calculated for other rotamers of 1PT by using the force field initially developed for the $^1P_H{}^2P_H$ rotamer and adjusting the torsional angles accordingly. Similar procedures were employed for 2M1PT and L-cysteine.

Since L-cysteine, 2M1PT, and 1PT have very low symmetry, we employed linear combinations of internal displacement coordinates and defined valence force constants corresponding to the idealized local symmetries of the CH_3, CH_2, NH_3^+, and COO^- groups, as appropriate. This procedure permits computation of the potential energy distribution (PED) in terms of accepted valence forces of the groups and simplifies the choice of force constants representing interaction between bonded atoms and nonbonded atoms. Local symmetry coordinates were transferred from appropriate amino acids and propane derivatives.[22-27] Diagonal and off-diagonal force constants are listed in Tables II and III, respectively. The torsional force constant about the C–S bond was determined for 1PT and 1PT-d_1 by using data from ethanethiol and ethanedeuteriothiol,[28,29] since the corresponding low-frequency infrared and Raman bands were not observed. The choice of interaction constants is based upon previous studies of alkanethiols[27] and L-cysteine.[24] Additional interaction terms were incorporated into the F matrix to obtain the best overall results for all molecules studied. Initial values for diagonal and off-diagonal force constants of 1PT, 2M1PT, 1PT-d_1, and L-cysteine were transferred from the work of Scott et al.[27] and Susi et al.[24] Initial refinements involved only diagonal force constants; subsequent refinements included the more sensitive off-diagonal terms. These refinements were continued until experimental and calculated frequencies were in good agreement.

Results

In this section we present both experimental (Raman) and calculated vibrational frequencies of L-cysteine and selected model mercaptans. Representative Raman spectra are shown for L-cysteine in the crystal and in aqueous solution, and for chromatographically pure 1-propanethiol liquid in nondeuterated and S-deuterated forms. Illustrations of experimental data not included

(18) Kerr, K. A.; Ashomore, J. P.; Koetzle, T. F. *Acta Crystallogr.* **1975**, *B31*, 2022–2026.
(19) Kojima, T. *J. Phys. Soc. Jpn.* **1960**, *15*, 1284–1291.
(20) Byler, D. M.; Gerasimowicz, W. V. *J. Mol. Struct.* **1984**, *112*, 207–219.
(21) Blom, C. E.; Altona, C. *Mol. Phys.* **1976**, *31*, 1377–1391.
(22) Destrade, C.; Garrigou-Lagrange, C.; Forel, M. T. *J. Mol. Struct.* **1971**, *10*, 203–219.
(23) Susi, H.; Byler, D. M. *J. Mol. Struct.* **1980**, *63*, 1–11.
(24) Susi, H.; Byler, D. M.; Gerasimowicz, W. V. *J. Mol. Struct.* **1983**, *102*, 63–79.
(25) King, W. T.; Crawford, B., Jr. *J. Mol. Spectrosc.* **1960**, *5*, 421–444.
(26) Pulay, P.; Fogarasi, G.; Pang, F.; Boggs, J. E. *J. Am. Chem. Soc.* **1979**, *101*, 2550–2560.
(27) Scott, D. W.; El-Sabban, M. Z. *J. Mol. Spectrosc.* **1969**, *30*, 317–337.
(28) Durig, J. R.; Bucy, W. E.; Wurrey, C. J.; Carreira, L. A. *J. Phys. Chem.* **1975**, *79*, 988–993.
(29) Richter, W.; Schiel, D. *Chem. Phys. Lett.* **1984**, *108*, 480–483.

Table IV. Experimental and Calculated Frequencies and Potential Energy Distributions for Normal Modes of L-Cysteine and Model Mercaptans[a]

exptl	calcd	dif	PED	exptl	calcd	dif	PED	exptl	calcd	dif	PED
					1PT ($^1P_H{}^2P_H$)						
2967	2965	2	r(99)	1453	1450	3	α(40), δ(56)	923	930	−7	β(77), R(10)
2967	2964	3	r(98)	1435	1434	1	δ(74), α(13)	896	885	11	β(90)
2932	2937	−5	d(98)	1381	1383	−2	δ(96)	816	830	−14	ϵ(90)
2932	2932	0	d(99)	1336	1333	3	W(93)	772	765	7	p(50), β(19)
2874	2877	−3	d(96)	1295	1297	−2	W(82)	650	654	−4	R′(88)
2874	2871	3	d(94)	1248	1246	2	T(97)	413	415	−2	w(78)
2856	2858	−2	r(95)	1217	1209	8	T(95)	284	285	−1	τ(76), P(20)
2581[b]	2580	1	t(93)	1109	1107	2	β(98)	240	245	−5	τ(42), Γ(36)
1461	1466	−5	δ(50), α(37)	1068	1063	5	β(98)	191[c]	191	0	τ'(95)
1453	1453	0	α(98)	1034	1033	1	R(98)	137	124	13	Γ(92)
					1PT ($^1P_C{}^2P_H$)						
2967	2965	2	r(99)	1453	1451	2	α(97)	923	927	−4	R(42), β(57)
2967	2964	3	r(98)	1435	1419	16	δ(82), α(12)	876	899	−23	β(94)
2932	2938	−6	d(98)	1381	1395	−14	α(89)	792	836	−44	ϵ(75)
2932	2930	2	d(99)	1353	1354	−1	W(99)	732	772	−40	p(44), ϵ(29)
2874	2880	−6	d(96)	1295	1286	9	W(88), p(12)	704	700	4	R′(72), β(15)
2874	2870	4	d(94)	1248	1256	−8	T(99)	361	358	3	w(72), R(20)
2856	2858	−2	r(94)		1176		T(89)	284	287	−3	τ(96)
2581[b]	2580	1	t(93)		1139		β(91)		211		P(91)
1461	1469	−8	α(40), δ(44)	1088	1083	5	β(98)	191[c]	189	2	τ'(98)
1453	1452	1	α(63), δ(32)	1034	1024	10	R(96)	137	134	3	Γ(96)
					1PT-d_1 ($^1P_H{}^2P_H$)						
2964	2965	−1	r(99)	1457	1449	8	δ(60), α(36)	899	925	−26	β(89)
2964	2964	0	r(98)	1434	1434	0	δ(71), α(12)	890	882	8	β(95)
2933	2938	−5	d(98)	1379	1383	−4	α(98)	793	785	8	p(50), β(38)
2933	2932	1	d(99)	1334	1333	1	W(96)	655	653	2	R′(76)
2874	2872	2	d(95)	1294	1295	−1	W(95)	617	599	18	ϵ(98)
2874	2868	6	d(98)	1244	1246	−2	T(98)	412	414	−2	w(80)
2856	2858	−2	r(95)	1213	1207	6	T(96)	282	282	0	τ(83)
1876[b]	1877	−1	t(95)	1098	1107	−9	β(98)	240	243	−3	P(90)
1457	1466	−9	α(45), δ(43)	1058	1061	−3	β(97)	150[c]	151	−1	τ'(98)
1457	1453	4	α(98)	1033	1033	0	R(98)	120	114	6	Γ(96)
					1PT-d_1 ($^1P_C{}^2P_H$)						
2964	2965	−1	r(99)	1457	1450	7	α(34), δ(58)	899	925	−26	R(47), β(52)
2964	2964	0	r(98)	1434	1419	15	δ(82), α(12)	854	894	−40	β(92)
2933	2938	−5	d(98)	1379	1396	−17	W(89)	730	799	−69	p(42), β(58)
2933	2930	3	d(99)	1353	1354	−1	W(82), α(12)		700		R′(70)
2874	2874	0	d(95)	1294	1283	11	T(88)	617	597	20	ϵ(99)
2874	2867	7	d(98)	1244	1256	−12	T(99)	361	356	5	w(76)
2856	2858	−2	r(94)		1176		β(87)	282	286	−2	τ(96)
1876[b]	1877	−1	t(95)		1135		β(92)		207		P(90)
1457	1469	−12	α(70), δ(30)	1082	1083	−1	β(98)	150[c]	142	8	τ'(98)
1457	1452	5	α(98)	1033	1024	9	R(96)	120	133	−13	Γ(93)
					L-Cysteine						
3167	3174	−7	r′(99)	1576	1562	14	α'(96)	1068	1084	−16	β'(37), β(50)
3167	3150	17	r′(99)	1527	1538	−11	α'(97)	1004	1002	2	β''(55), β(21)
3055	3064	−9	r′(99)	1427	1432	−5	δ(96)	943	948	−5	β'(94)
2998	2952	46	d(99)	1400	1409	−9	T′(25), R″(60)	943	933	10	β'(21), β(51)
2960	2945	15	d(99)	1351	1339	12	W(74), α'(25)	870	871	−1	Ω(93)
2918	2913	5	d(96)	1300	1295	5	β'''(56), T′(23)	825	833	−8	p(61)
2582[d]	2586	4	t(96)	1273	1268	5	T(42), T′(20)	773	763	10	ϵ(95)
1616	1624	−8	α'(56), T′(34)	1201	1158	43	β'(17), T(65)	696	698	−2	R′(95)
1616	1608	8	T′(69), α'(22)	1110	1094	16	β(89), R‴(10)	642	643	−1	ϕ(31), R‴(26)

[a] Abbreviations: 1PT, 1-propanethiol; 1PT-d_1, 1-propanedeuteriothiol; exptl, experimental frequency (cm^{-1}); calcd, calculated frequency (cm^{-1}); dif = exptl − calcd; PED, calculated potential energy distribution (as defined in the Materials and Methods); r, α, β, and τ denote C–H stretching, HCH bending, rocking, and torsion, respectively, of the CH_3 group; d, δ, W, T, P, and w denote C–H stretching, HCH bending, wagging, twisting, CCS bending, and CCC bending, respectively, of the CH_2 group; t, ϵ, and p denote S–H stretching, CSH(D) bending, and HCS bending, respectively, of the sulfhydryl moiety; R, R′, Γ and τ' denote C–C stretching, C–S stretching, C–C torsion and C–S torsion, respectively, of the propyl main chain; r′, α', β', β'', Θ and τ'' denote N–H stretching, HNH bending, HNC bending, NCH bending, CCN bending, and torsion, respectively, of the NH_3^+ group; T, ϕ, ϕ', Θ′, β''', and Ω denote C–O stretching, CCO bending, OCO bending, NCC bending, CCH bending, and C–COO out-of-plane bending, respectively, of the COO^- group; and R″, R‴, and Γ′ denote C_α–COO stretching, C_α–N stretching, and C_α–COO torsion, respectively, of cysteine. Rotamer notation is defined in Figure 1. [b] Data from 1% 1PT and 1PT-d_1 solutions (mol/mol) in CCl_4. [c] Data from ethanethiol and ethanedeuteriothiol (ref 28). [d] Data from 1% L-cysteine solution (mol/mol) in H_2O.

in the figures (spectra of 7 compounds) are available as supplementary material.

Raman spectra of neat liquids 1-propanethiol (1PT) and 1-propanedeuteriothiol (1PT-d_1) in the region 300–3200 cm^{-1} are compared in Figure 2A. The Raman data have not been published previously, although a portion of the 1PT spectrum has been reported.[27] The computed difference spectrum of Figure 2A (1PT-d_1 minus 1PT) shows that sulfhydryl deuteration displaces several bands of the 300–1000-cm^{-1} region in addition to the expected large shift of the sulfhydryl stretching mode (σ_{SH}/σ_{SD} = 2570/1868 = 1.376). (In the Discussion and Tables IV and V, we report data obtained from dilute CCl_4 solutions rather than neat liquids, in order to avoid effects of hydrogen bonding on σ_{SH} or σ_{SD}). Experimental frequencies of 1PT isotopomers are listed in Table IV. Included in Table IV are the calculated vibrational frequencies and corresponding potential energy distributions (PED)

Table V. Experimental and Calculated Frequencies and Potential Energy Distributions of C–S and S–H Modes of L-Cysteine and Model Mercaptans[a]

		σ_{SH} (σ_{SD})				σ_{CS}			
molecule	rotamer[b]	exptl[c]	calcd	dif	PED	exptl[d]	calcd	dif	PED
1PT	$^1P_H{}^2P_H$	2581	2580	1	93	650	654	−4	88
	$^1P_H{}^2P_C$	2589	2595	−6	93	650	646	4	89
	$^1P_C{}^2P_H$	2581	2580	1	93	704	700	4	72
	$^1P_C{}^2P_C$	2589	2595	−6	93	704	698	6	68
1PT-d_1	$^1P_H{}^2P_H$	(1876)	(1877)	−1	95	655	653	2	76
	$^1P_H{}^2P_C$		(1899)		94		666		69
	$^1P_C{}^2P_H$	(1876)	(1877)	−1	95		702		70
	$^1P_C{}^2P_C$		(1899)		94		699		62
2M1PT	$^1P_H{}^2P_C$	2589	2595	−6	93	667	665	2	73
	$^1P_H{}^2P_H$	2581	2580	1	94	667	661	6	77
	$^1P_C{}^2P_C$	2589	2595	−6	93	712	714	−2	54
	$^1P_C{}^2P_H$	2581	2580	1	94	712	714	−2	53
L-Cys	$^1P_H{}^2P_H$	2582[e]	2586	−4	96	696[f]	698	−2	95
	$^1P_C{}^2P_H$		2586				734		90
	$^1P_N{}^2P_H$		2586				738		90

[a] Abbreviations and notation are defined in the footnote of Table IV. [b] Rotamers are depicted in Figure 1. [c] Dilute CCl_4 solutions (1% mol/mol). [d] Neat liquids. [e] Aqueous solution (1% mol/mol). [f] Orthorhombic crystal.

for the principal rotamers of 1PT and 1PT-d_1. Typical rotamers ($^1P_H{}^2P_H$ and $^1P_C{}^2P_H$) are illustrated in Figure 1C and defined in the caption. Raman spectra obtained on crystal and solution forms of L-cysteine are shown in Figure 2B. Experimental and calculated frequencies of L-cysteine, their differences, and their calculated potential energy distributions also are listed in Table IV. The sulfhydryl stretching (σ_{SH}) and carbon–sulfur stretching (σ_{CS}) modes of all compounds are summarized in Table V.

Discussion

1. 1-Propanethiol (1PT) and 1-Propanedeuteriothiol (1PT-d_1). The vibrational assignment presented here for 1PT and 1PT-d_1 (Table I) resolves a number of discrepancies between those previously proposed for this molecule by Scott and El-Sabban[27] and Hayashi et al.[30] Our assignment is also in excellent agreement with that proposed for *n*-propyl chloride by Shimanouchi and co-workers.[31] Furthermore, our assignment satisfies the Rayleigh noncrossing rule for these two isotopomers and fits the Teller–Redlich product rule to within 4.8% (with transfer of SH torsional frequencies from ethanethiol and ethanethiol-S-d_1,[28] to approximate those not observed in the present spectra). The majority of the vibrational frequencies of 1PT and 1PT-d_1 are attributed to the $^1P_H{}^2P_H$ conformer for the reasons discussed previously and in the following paragraph. Other bands, which exhibit temperature-dependent relative intensities, are assigned to the $^1P_C{}^2P_H$ rotamer. In a subsequent section, we discuss the existence of ^2P_C conformers.

Of particular note in assigning observed vibrational bands to specific conformers is the 361–413-cm^{-1} doublet (Figure 2A). Both the present normal coordinate analysis and previous work on *n*-propyl chloride[31] attribute the doublet to C–C–C bending. A van't Hoff plot showing the logarithmic dependence of relative band intensities on reciprocal temperature is given in Figure 3. These results demonstrate that, even though the ^1P_C conformer gives rise to the more intense component of the doublet (361 cm^{-1}), the ^1P_H conformer is more stable by 0.67 ± 0.10 kcal/mol, which is also in accordance with the data on *n*-propyl chloride.[31] Thus, we attribute ^1P_H as the predominant conformer about X^1, and based upon arguments given by Li and Thomas,[1] we attribute ^2P_H as the predominant conformer about X^2. The observed frequencies are assigned to the $^1P_H{}^2P_H$ (major) and $^1P_C{}^2P_H$ (minor) conformers, with contributions from ^2P_C conformers evidenced only in the sulfhydryl stretching region, as discussed in the next section.

Based upon these assignments, a force field was determined for 1PT and 1PT-d_1 using the 33 force constants shown in Tables II and III. This force field fit the observed vibrational frequencies of $^1P_H{}^2P_H$ isotopomers to an average error of approximately 6 cm^{-1}. Since the average error is so small, no further attempts were made to improve this fit by incorporating additional force constants in the force field.

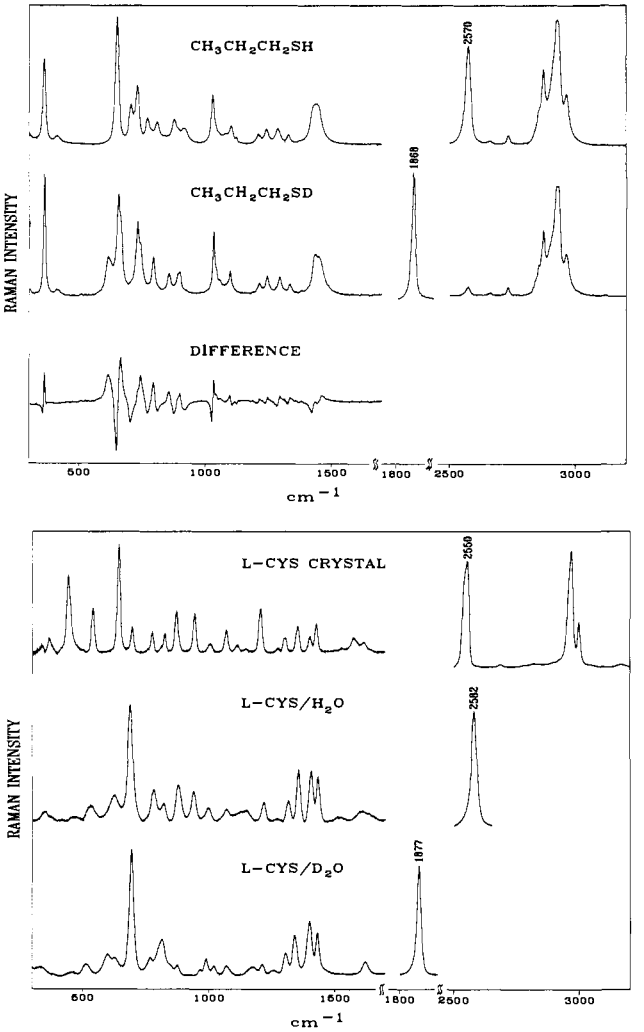

Figure 2. (A) Raman spectra in the region 300–3200 cm^{-1} of 1-propanethiol (1PT) and 1-propanedeuteriothiol (1PT-d_1) and their corresponding difference spectrum (1PT-d_1 minus 1PT). Data are from neat liquid samples at 25 °C. (B) Raman spectra of L-cysteine orthorhombic crystal (top), H_2O solution at pH 7 (middle), and D_2O solution at pD 7 (bottom).

(30) Hayashi, M.; Shiro, Y.; Murata, H. *Bull. Chem. Soc. Jpn.* **1966**, *39*, 112–117.

(31) Ogawa, Y.; Imazeki, S.; Yamaguchi, H.; Matsuura, H.; Harada, I.; Shimanouchi, T. *Bull. Chem. Soc. Jpn.* **1978**, *51*, 748–767.

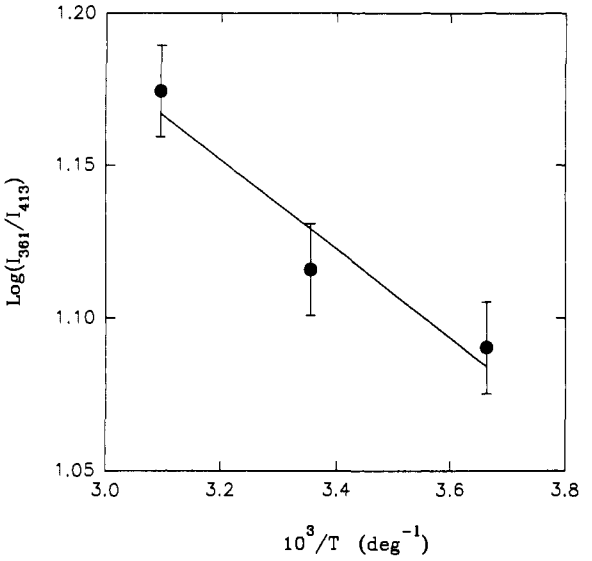

Figure 3. Semilogarithmic plot of the rotamer concentration ratio ($^1P_C/^1P_H$), represented by the quotient of Raman intensities (I_{361}/I_{413}) in the spectrum of liquid 1-propanethiol, versus reciprocal temperature in the interval $0° \leq t(°C) \leq 50°$.

(a) Effect of the X^2 Torsion on σ_{SH}. Previously, we reported that the Raman S–H stretching (σ_{SH}) band in spectra of CCl_4 solutions of 1-propanethiol (1PT), 2-propanethiol (2PT), and 2-methyl-1-propanethiol (2M1PT) is unsymmetrical, while that of 2-methyl-2-propanethiol (2M2PT) is symmetrical.[1] Since only the last compound is incapable of rotational isomerism involving the C_α–C_β–S–H network (torsion angle X^2), the asymmetric σ_{SH} band of each of the former compounds was attributed to a low population of a minor rotamer, deduced by analogy with ethanethiol to be the ^2P_C rotamer.[28,29] In each asymmetrically C_α-substituted thiol, σ_{SH} could be decomposed into an intense component (^2P_H rotamer) separated by 8–10 cm^{-1} from the weak component (^2P_C rotamer), also consistent with the reported 9-cm^{-1} difference between σ_{SH} bands of ethanethiol rotamers. We have now confirmed the same pattern of bandshapes for CCl_4 solutions of deuteriothiols, i.e., the σ_{SD} bands of 1PT-d_1 (1876 cm^{-1}) and 2M2PT-d_1 (1872 cm^{-1}) are, respectively, asymmetrical and symmetrical (data not shown). This suggests that the minor band components are not the fortuitous result of overtone or Fermi contributions. Further, the gas-phase FTIR spectra of 1PT, 2M1PT, and 2PT reveal two overlapping S–H stretching bands, while that of 2M2PT shows a single band, in full accord with the Raman results. The consistency between Raman and IR bands also supports the multiple rotamer assignments.

In order to understand the dependence of σ_{SH} (and σ_{SD}) upon rotational isomerism, we conducted normal coordinate calculations on ^2P_H and ^2P_C rotamers of 1PT (and 1PT-d_1). When the refined force constants (Tables II and III) obtained from the normal mode analysis of the ^2P_H rotamer of 1PT were fixed and the intramolecular geometry was changed from ^2P_H to ^2P_C, we found that σ_{SH} increased by 15 cm^{-1} for 1PT and by 21 cm^{-1} for 1PT-d_1. These calculated frequency shifts are consistent with the experimental results and provide support for the postulated dependence of σ_{SH} upon rotational isomerism, including assignment of the higher σ_{SH} mode to the ^2P_C rotamer. Also, the normal mode analysis shows that the mixing among the off-diagonal force constants [$f(34)$, $f(41)$, $f(42)$, and $f(43)$, Table III] accounts mostly for the conformation dependence of σ_{SH}. Thus, σ_{SH} is not a completely pure S–H stretching mode; the potential energy distribution indicates 93% S–H stretching, 5% C–H stretching, 1% ∠CSH bending, and 1% ∠SCH bending. Nominally lesser mixing is observed for the deuterio derivative.

(b) Effects of the X^1 and X^2 Torsions on σ_{CS}. Correlations between the Raman C–S stretching frequency (σ_{CS}) and C_α–C_β torsions (X^1) in disulfides and thioethers are well-known.[11] Our studies show that both 2M1PT and 1PT (neat liquids) display

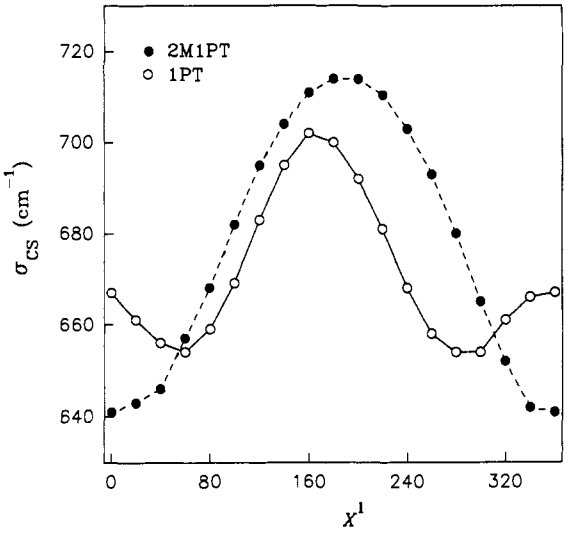

Figure 4. Dependence of the C–S stretching frequencies of 1-propanethiol (○) and 2-methyl-1-propanethiol (●) on the C–C–C–S dihedral angle (X^1).

two bands in the C–S stretching region (600–800 cm^{-1}), indicating an equilibrium of two X^1 rotamers for each mercaptan. The more intense band near 650 cm^{-1} is assigned to the ^1P_H rotamer, and the weaker band near 704 cm^{-1} is assigned to the ^1P_C rotamer, as reported previously.[30] Normal coordinate analysis of 1PT indicates that by fixing the refined force constants (Tables II and III) and changing the intramolecular geometry from ^1P_H to ^1P_C, σ_{CS} increases by about 46 cm^{-1}. This calculated result is in excellent agreement with the experimentally observed rotamer shift of 54 cm^{-1} (data not shown). On the other hand, σ_{CS} is much less affected (<10 cm^{-1}) by changes in the C_β–S torsion (X^2).

The calculated dependence of σ_{CS} on X^1 is shown for 1PT in Figure 4. This plot of σ_{CS} vs X^1 is clearly seen to be symmetric. In the interval $0° < |X^1| < 60°$, σ_{CS} is virtually invariant; however, for $60° < |X^1| < 180°$, σ_{CS} varies significantly.

(c) Other Vibrational Modes. Carbon–hydrogen stretching vibrations of CH_3 and CH_2 groups are not expected to vary significantly with rotational isomerism, since the frequencies depend almost exclusively on C–H stretching force constants [$f(3)$ and $f(4)$, Table II]. We note that the experimental C–H stretching frequencies are also subject to larger uncertainty than other frequencies (Figure 2) because of the extensive band overlap, the relatively low spectral resolution employed, and the effects of Fermi resonance. Nevertheless, the experimental data (Table IV) are in accord with anticipated group frequencies.[32] For C–H bending and C–C stretching modes, which are largely rotamer independent, the experimental and calculated results are also in good agreement (average error < 8 cm^{-1}).

2. 2-Methyl-1-propanethiol (2M1PT). The 30 frequencies observed for the various rotamers of 2M1PT were calculated with an average error of 15 cm^{-1} using the 33 force constants transferred from 1PT, plus four interaction force constants [$f(49)$, $f(50)$, $f(51)$, and $f(52)$, Table III].

As noted previously,[1] the Raman S–H stretching band of 2M1PT in CCl_4 solution is asymmetrical, which implies the coexistence of two rotamers (^2P_C and ^2P_H). Normal coordinate analysis of 2M1PT, using force constants transferred from 1PT, confirms that a change of intramolecular geometry from ^2P_C to ^2P_H shifts σ_{SH} from 2595 to 2580 cm^{-1} (Table V), consistent with the experimental results.[1] The conformational dependence of σ_{SH} is similar for 2M1PT and 1PT.

The ^1P_H and ^1P_C rotamers of 2M1PT exhibit σ_{CS} modes at 667 and 712 cm^{-1}, respectively.[33] Normal coordinate calculations using only the force constants transferred from 1PT do not re-

(32) Bellamy, L. J. *The Infrared Spectra of Complex Molecules*, 3rd ed.; Chapman and Hall: London, 1975; Vol. I.
(33) Ozaki, Y.; Sugeta, H.; Miyazawa, T. *Chem. Lett.* **1975**, 713–716.

produce these frequencies acceptably (average error > 35 cm^{-1}), in part because of the change in major rotamer from ^1P_H in 1PT to ^1P_C in 2M1PT.[33] Additional interaction force constants [$f(49)$, $f(50)$, $f(51)$, and $f(52)$] are required to improve agreement between experimental and calculated frequencies to an average error of 15 cm^{-1}, as given in Table III. With the additional force constants, the ^1P_H to ^1P_C conformation change of 2M1PT increases the calculated σ_{CS} by 49 cm^{-1}, which approximates quite well the observed increase of 45 cm^{-1}. The assignments for other vibrational modes are in good agreement with those for 1-chloro-2-methylpropane.[34] The better agreement achieved between the observed and calculated σ_{CS} values of 1PT is attributed to its lack of a C_α methyl substituent which significantly simplifies the corresponding force field. For 2M1PT, the correlation of σ_{CS} with X^1 is also plotted in Figure 4. Neglect of the above noted interaction force constants elevates the σ_{CS} frequencies less than 15 cm^{-1} and does not change the shape of the Figure 4 plot. The calculated dependence of σ_{CS} on X^2 is marginal (<5 cm^{-1}), as shown in Table V.

Other calculated and experimental frequencies of 2M1PT are acceptable. Average errors are less than 20 cm^{-1}. The experimental results and normal coordinate calculations on 2M1PT permit identification of conformation-sensitive interaction force constants which are likely transferable to L-cysteine (next section).

3. L-Cysteine. Although L-cysteine contains C_α carboxyl and amino substituents, the force constants transferred from 1PT permit calculation of L-cysteine vibrational frequencies in good agreement with the experimental results (Table IV). Our vibrational assignments are also in good agreement with those of Susi et al.[24] In the frequency region above 600 cm^{-1}, the average error is 15 cm^{-1}, which indicates that the stretching and bending force constants are reasonably transferable from 1PT. Below 600 cm^{-1} the average error is larger, which is consistent with the expectation that carboxyl and amino group substituents at C_α should alter interaction (off-diagonal) force constants. Further resolution of the low-frequency assignments will require additional data from appropriate amino acid analogues.

By using the force constants transferred from 1PT and by changing the conformation of L-cysteine from the observed ^1P_H rotamer to either ^1P_C or ^1P_N, σ_{CS} can be predicted to increase by 36–40 cm^{-1}. This correlation may be useful for determining the cysteine side-chain conformation in proteins.

Conclusions

Using a generalized valence force field, we have calculated the normal modes of vibration of 1-propanethiol and 1-propanethiol-d_1 to a high degree of accuracy. We have determined that the set of refined force constants developed for 1PT and 1PT-d_1 is satisfactorily transferable to 2-methyl-1-propanethiol and L-cysteine. The latter two compounds serve as models representing the cysteine side chain of proteins. We expect the force field developed in this work to also provide a basis for accurately reproducing the vibrational frequencies of other mercaptans and structurally related cysteine analogues.

An important conclusion reached from previous empirical studies[1] is that the Raman S–H stretching frequency of cysteine derivatives is weakly dependent upon the conformation of the C_α–C_β–S–H side chain. The present normal coordinate calculations confirm the earlier conclusion and indicate that this conformation dependence originates through minor potential energy contributions to the normal mode from C_α–H stretching (5%), C_β–S–H bending (1%), and H–C_β–S bending (1%). Thus, although changes in the skeletal torsion X^2 alone may shift σ_{SH}, the maximum conformational shift is observed (<10 cm^{-1}) and predicted (<15 cm^{-1}) to be small in comparison to the maximum frequency shift (≈60 cm^{-1}) resulting from hydrogen bonding by the S–H donor.[1]

In accordance with experimental findings on C–S stretching modes in model sulfides,[11] our calculations predict that the analogous cysteine normal mode (σ_{CS}, involving mainly C_β–S stretching) is highly sensitive to rotation about the C_α–C_β bond (X^1 torsion). For typical ^1P_H and ^1P_C rotamers, σ_{CS} is calculated to differ by as much as 30–50 cm^{-1}, which is consistent with the experimental results. Since σ_{CS} is highly sensitive to values of X^1 in the interval $60° < |X^1| < 180°$ (Figure 4), we conclude that measurements of σ_{CS} from Raman spectra will provide a convenient means for estimating the C_α–C_β torsional angle and for determining the cysteine side-chain conformation in proteins.

In summary, the present studies demonstrate a specific structural basis for dependence of the Raman S–H stretching frequency upon torsion angle X^2, and a specific structural basis for dependence of the Raman C–S stretching frequency upon torsion angle X^1 (Figure 1). The present results should permit the experimental Raman frequencies to be interpreted in terms of cysteine side-chain geometry in proteins.

Together with previous results,[1] the analysis given here shows that the Raman S–H stretching band may be exploited as an indicator of *both SH hydrogen bonding and intramolecular geometry*. With respect to hydrogen bonding, the study of aliphatic and aromatic mercaptans in both polar and apolar solvents and of L-cysteine and glutathione in the crystal have provided a basis for interpreting the S–H stretching region of the Raman spectrum in terms of hydrogen bond donation by S–H and hydrogen bond acceptance by S.[1,35] When the S–H group is not hydrogen-bonded, e.g., at high dilution in CCl_4, $\sigma_{SH} \approx 2585 \pm 5$ cm^{-1}. This S–H frequency is lowered by 25–60 cm^{-1} for strong S–H donors, 10–25 cm^{-1} for moderate S–H donors, and 5–10 cm^{-1} for weak S–H donors. On the other hand, hydrogen bond acceptance by S, in the absence of S–H donation, elevates σ_{SH} slightly (≈4 cm^{-1}). The effect of intramolecular geometry upon σ_{SH} is always small (<10 cm^{-1}). We also note that since hydrogen bonding greatly affects the Raman S–H bandwidth, a small change in hydrogen-bonding strength can be distinguished from a conformational change by the effect of the former upon the experimentally observed Raman bandwidth.

Acknowledgment. The support of this research by the U.S. National Institutes of Health (Grant AI11855) is gratefully acknowledged. We thank Professor Richard Mathies (U.C. Berkeley) for sharing the normal coordinate program GZINT and Dr. Tom Pollard for assistance with its installation. We also thank Professor Andrew H.-J. Wang (U. Illinois, Urbana–Champaign) for verifying crystal structures of model mercaptans by X-ray diffraction and Professor Issei Harada (Tohoku University, Sendai, Japan) for helpful comments to improve the manuscript.

Supplementary Material Available: Figures S1 and S2 giving Raman spectra of anhydrous liquid mercaptans in the region 300–2650 cm^{-1} and of single crystals and H_2O and D_2O solutions of glutathione (GSH) in the region 300–2565 cm^{-1} (3 pages). Ordering information is given on any current masthead page.

(34) Crowder, G. A.; Lin, W.-Y. *J. Mol. Struct.* **1980**, *64*, 193–199.

(35) Li, H.; Benevides, J. M.; Thomas, G. J., Jr. *Biophys. J.* **1991**, *59*, 110a.